Naval Research Laboratory

Washington, DC 20375-5000

AD-A187 541

Debris Charge States in HANE and in the NRL Laser Experiment

E. HYMAN

Science Applications International Corporation
McLean, Virginia 22101

M. MULBRANDON AND J. L. GIULIANI, JR.

Geophysical and Plasma Dynamics Branch
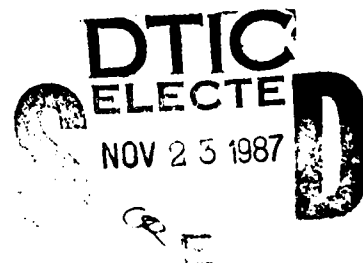*Plasma Physics Division*

October 30, 1987

DTIC
ELECTE
NOV 2 3 1987
D

AD-A187541

REPORT DOCUMENTATION PAGE

1a. REPORT SECURITY CLASSIFICATION UNCLASSIFIED	1b. RESTRICTIVE MARKINGS
2a. SECURITY CLASSIFICATION AUTHORITY	3. DISTRIBUTION/AVAILABILITY OF REPORT Approved for public release; distribution unlimited.
2b. DECLASSIFICATION/DOWNGRADING SCHEDULE	
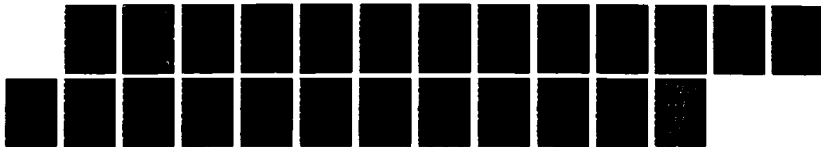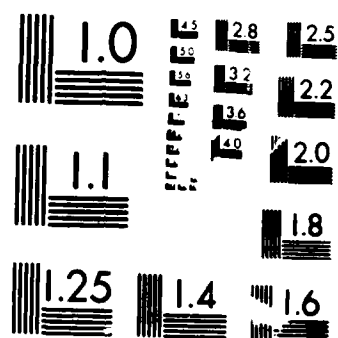
4. PERFORMING ORGANIZATION REPORT NUMBER(S) NRL Memorandum Report 6085	5. MONITORING ORGANIZATION REPORT NUMBER(S)

6a. NAME OF PERFORMING ORGANIZATION Naval Research Laboratory	6b. OFFICE SYMBOL (If applicable) Code 4780	7a. NAME OF MONITORING ORGANIZATION
6c. ADDRESS (City, State, and ZIP Code) Washington, DC 20375-5000		7b. ADDRESS (City, State, and ZIP Code)

8a. NAME OF FUNDING/SPONSORING ORGANIZATION Defense Nuclear Agency	8b. OFFICE SYMBOL (If applicable) RAAE	9. PROCUREMENT INSTRUMENT IDENTIFICATION NUMBER 47-0889-07 (MIPR No. 87-518)

8c. ADDRESS (City, State, and ZIP Code) Washington, DC 20305	10. SOURCE OF FUNDING NUMBERS			
	PROGRAM ELEMENT NO. 62715H	PROJECT NO. S99QMXBC –	TASK NO. 00102	WORK UNIT ACCESSION NO. DN580-072

11. TITLE (Include Security Classification)
    Debris Charge States in Hane and in the NRL Laser Experiment

12. PERSONAL AUTHOR(S)
    Hyman*, E., Mulbrandon, M. and Giuliani, J.L., Jr.

13a. TYPE OF REPORT Interim	13b. TIME COVERED FROM _____ TO _____	14. DATE OF REPORT (Year, Month, Day) 1987 October 30	15. PAGE COUNT 23

16. SUPPLEMENTARY NOTATION
    *This report was sponsored by DNA under "Weapons Phenomenology and Code Development."
    Work Unit Code and Title: RB RC/00158, Plasma Structure Evolution.

17	COSATI CODES		18. SUBJECT TERMS (Continue on reverse if necessary and identify by block number)
FIELD	GROUP	SUB-GROUP	HANE (High Altitude Nuclear Explosion) NRL, Laser Experiment, Debris Charge State, Scaling, Recombination Rates

19. ABSTRACT (Continue on reverse if necessary and identify by block number)

We show that in the NRL laser experiment the expanding debris ions remain highly charged, in contrast to the situation in a high altitude nuclear explosion (HANE) in which recombination to a low charge state is rapid. The difference in the two cases is a result of (1) a failure in the scaling of debris density relative to a HANE in the early expansion phase and (2) a failure in scaling of the energy deposition time. Results based on simple idealized models for the HANE and laser experiment are presented and these are compared with more sophisticated calculations.

20. DISTRIBUTION/AVAILABILITY OF ABSTRACT ☒ UNCLASSIFIED/UNLIMITED ☐ SAME AS RPT. ☐ DTIC USERS	21. ABSTRACT SECURITY CLASSIFICATION UNCLASSIFIED	
22a. NAME OF RESPONSIBLE INDIVIDUAL J.D. HUBA	22b. TELEPHONE (Include Area Code) 202-767-3630	22c. OFFICE SYMBOL Code 4780

DD FORM 1473, 84 MAR

83 APR edition may be used until exhausted.
All other editions are obsolete.

i

CONTENTS

Accession For

NTIS GRA&I

DTIC TAB

Unannounced

Justification

By

Distribution/

Availability Codes

Dist | Avail and/or
     | Special

A-1

DTIC

COPY

INSPECTED

8

DEBRIS CHARGE STATES IN HANE AND
IN THE NRL LASER EXPERIMENT

I. Introduction

It is reasonably well established that the charge state, z, of HANE debris drops from very high values to z close to 1 on disassembly time scales. Both observations and disassembly calculations suggest this result. A calculation by Clark and Jacobs at NRL[1] estimates that the charge state drops to z ~ 1 by the time the burst has expanded to ~ 200 meters radius, at which point the charge state is frozen in. That is, by this time the density has dropped to the point that recombination is too slow to be important and, further, future temperature decreases will not be sufficient to increase the recombination coefficient enough to offset the density decrease.

At the Naval Research Laboratory a laser target experiment, PHAROS II[2], has been designed and operated to model on a reduced scale some of the physics occuring in an actual HANE. Simulations of the laser experiment using a hydro-chemistry-radiation code HANEX[3] predict very high charge states (z ~ 10) for the laser experiment in the forward moving debris, which persist, at least, until interaction with the background gas becomes important. We have identified two critical differences between the laser experiment and the HANE event that are responsible for the disparity in the results:

(1) a failure in density scaling in the adiabatic expansion phase, and

(2) a difference in scaled times for the deposition of the laser/nuclear energy, during disassembly.

The laser experiment was designed to scale relative to HANE in the following way, [4]

$$t_H = 10^6 t_L$$
$$r_H = 10^6 r_L$$
$$n_H = 10^{-6} n_L \qquad (1)$$
$$M_H = 10^{12} M_L$$
$$E_H = 10^{12} E_L$$

where t, r, n, M, and E are respectively time, expansion radius, background density, debris mass, and energy for HANE (H) and the laser experiment (L). It follows from Eq. 1, that 2-body reaction rate time scales should be related by $\tau_H = 10^6 \tau_L$ (since $\tau = (n\alpha)^{-1}$, where α is the rate coefficient).

In this note, we will show that there is a breakdown in scaling, and that recombination is much less effective in the laser experiment than it is in HANE, with the result that the laser debris remains highly charged. In Section II we will show that during the debris expansion, recombination times are the same in HANE and in the laser experiment (they do not scale, as suggested by Eq. 1). Also, "problem time" scales like 10^4, not 10^6, during the expansion, as we will see. In Section III we introduce an idealized HANE model and an idealized model for the laser experiment to clarify the essential distinctions. In Section IV we compare these results with HANEX code calculations and present our conclusions.

II. Scaling and Debris Recombination

To evaluate the importance of recombination (or ionization) in reducing (increasing) the average charge state of the debris, it is convenient to introduce the dimensionless parameter, ξ, the fraction of ions that will recombine or ionize in a time interval δt

$$\xi = \frac{\delta t}{\tau} \qquad (2)$$

2

where $\tau = (N_e \alpha)^{-1}$, (N_e = electron density) is the recombination (ionization) time. In this discussion we neglect 3-body recombination, which is unimportant at the high temperatures associated with the early debris expansion. It is included in our model, however. We choose δt to be the time scale for changes in the density and temperature (an expansion time scale). Then the expanding plasma charge state will be in equilibrium if ξ for both recombination and ionization are large. If ξ becomes less than unity the plasma may no longer be in equilibrium. In particular, if ξ for recombination processes becomes and stays much less than unity, then that charge state will be frozen at its existing value, i.e., recombination will not occur.

If the debris expansion scaling satisfied Eq. 1, then according to Eq. 2, ξ for HANE and the laser experiment would be the same. However, this is not the case for debris recombination during the early expansion of the debris. Here, the ambient density is negligible compared to the debris density. Both in the laser experiment and in the HANE the debris density starts from the solid state. Thus, debris density is not scaled at all in the expansion phase; it is the same for HANE and the laser.

If the laser experiment were strictly a scaled down HANE (mass scaled by 10^{-12}) with the same initial temperature, the time scale for recombination (and ionization), τ, would be identical. However, if mass (M) scales $\sim 10^{12}$, and because debris densities are the same, the expansion radius scales $\sim (M)^{1/3} \sim 10^4$. Since expansion velocities are comparable, time (δt) scales $\sim 10^4$, also. Then, from Eq. 2, <u>for HANE $\xi \sim 10^4$ times larger than in a laser experiment size HANE.</u>

In the real experiment the temperature of the debris never exceeds 10^3 eV, while in HANE the temperature is greater than 10^4 eV at early times. If the laser stayed cooler than in a HANE, increased recombination at lower temperatures might compensate somewhat for the ξ discrepancy. However, in

3

the HANE event, the energy is released and deposited in a time $\sim 10^{-6}$sec. In the laser, scaling of problem time by 10^{-4} implies an appropriate deposition time $\sim 10^{-10}$sec, but the actual deposition time is $\sim 10^{-8}$sec. Thus, there is a scaling discrepancy of order 10^{-2}. In other words, the laser energy is deposited over a time period a factor of 10^2 too long compared to a HANE. Thus, while the HANE debris is expanding adiabatically, and cooling accordingly, the laser debris expands but is maintained at a high temperature as long as the laser is on.[3] Thereafter, the debris expands and cools adiabatically but the temperature remains higher than in a HANE, at the same densities. This higher temperature also decreases recombination processes in the laser experiment.

Thus, recombination is less effective in the laser experiment, first, because of scaling which requires ξ_R(HANE) $= 10^4 \xi_R$(LASER) and, second, because the long laser energy deposition time delays cooling. In the next section we illustrate the result of these effects using simplified models for the HANE and the laser experiment.

III. Results

The recombination coefficient is made up of 3 parts: radiative recombination, dielectronic recombination, and 3-body recombination. Their general dependence with temperature is quite different and explains their relative importance in different regimes. At intermediate temperatures dielectronic recombination tends to be larger than radiative and 3-body is unimportant. Dielectronic falls off somewhat faster than radiative ($\sim T_e^{-3/2}$ vs. $\sim T_e^{-1}$) with increasing temperature. At lower temperatures dielectronic drops off exponentially while radiative continues to increase. At very low temperatures 3-body will dominate even at low densities because it increases like $T_e^{-9/2}$ as T_e decreases.[5] In Appendix I we present expressions for each of these rate coefficients.

4

Table 1 shows "typical" HANE parameters for ideal adiabatic expansion of aluminum into a vacuum. The plasma expands radially at constant velocity $v = 1 \times 10^8$ cm/sec, according to

$$n = n_0 (r_0/R)^3; \tag{3}$$

where $\qquad\qquad R = vt$

Assuming adiabatic expansion with $\gamma = 5/3$,

$$T = T_0 (r_0/R)^2 \tag{4}$$

T_0, M_0 and r_0 are the temperature, density, and radius when the expansion begins. Included in the Table are temperature (T), debris ion density (n),

TABLE 1

T (ev)	n (cm^{-3})	t (sec)	R (cm)	ξ_{R3}	ξ_{RR}	ξ_{RD}	ξ_I	z
1.0E+05	1.0E+23	1.0E-06	1.0E+02	0.0E+00	5.5E+04	-----	1.2E+07	13
2.2E+04	1.0E+22	2.2E-06	2.2E+02	0.0E+00	3.8E+04	-----	4.0E+06	13
4.6E+03	1.0E+21	4.6E-06	4.6E+02	7.4E+00	2.6E+04	-----	6.7E+05	13
1.0E+03	1.0E+20	1.0E-05	1.0E+03	2.3E+00	1.1E+04	2.5E+04	4.7E+04	12
2.2E+02	1.0E+19	2.2E-05	2.2E+03	1.7E+00	2.4E+03	4.5E+04	5.1E+04	10
4.6E+01	1.0E+18	4.6E-05	4.6E+03	2.7E+00	4.5E+02	1.3E+03	5.9E+03	6
1.0E+01	1.0E+17	1.0E-04	1.0E+04	1.9E+01	6.4E+01	5.0E+01	5.6E-01	4
2.2E+00	1.0E+16	2.2E-04	2.2E+04	9.2E+00	5.3E+00	9.1E+02	6.5E+01	2
4.6E-01	1.0E+15	4.6E-04	4.6E+04	8.5E+00	3.2E-01	2.0E+01	7.8E-01	1
1.0E-01	1.0E+14	1.0E-03	1.0E+05	4.4E+02	2.3E-01	6.3E-06	5.9E-18	1
2.2E-02	1.0E+13	2.2E-03	2.2E+05	4.9E+03	1.7E-01	0.0E+00	5.9E-19	1

time (t), and radial expansion (R). We have calculated the parameter, ξ, for 3-body recombination (ξ_{R3}), radiative recombination (ξ_{RR}), dielectronic recombination (ξ_{RD}), and ionization (ξ_I). The last column is the approximate value of the dominant charge state, z. In the calculation of ξ we have approximated the expansion time scale δt, by the problem time t, given in the Table. The parameters ξ are calculated assuming recombination from z to z - 1 and ionization from z - 1 to z. In a cooling plasma if at least one of the ξ's for recombination is greater than unity the plasma is in equilibrium and the charge state, z, is determined by the temperature, T.

At very early times the plasma is in equilibrium and is stripped. (Dielectronic recombination is not defined for a stripped ion.) As the adiabatic expansion continues and density and temperature drop, the plasma remains in equilibrium and the charge state begins to drop. Both dielectronic recombination and radiative recombination are important. Eventually, the temperature is sufficiently low that the charge state drops to z $\sim$ 1 (n $\sim$ 10^{15} cm^{-3}). At this time dielectronic and 3 body recombination are comparable. As density and temperature are reduced further (r $<$ 10^{15} cm^{-3}) 3-body recombination begins to dominate. Here, we need to stress that we have used a model of an ideal adiabatic expansion. In the real case, each recombination releases energy, much of which ends up heating the electrons. Thus, the plasma will no longer cool adiabatically and the temperature will not drop so precipitously. As the density continues to decrease below $\sim$ 10^{15} cm^{-3}, the debris is likely to be frozen at z close to 1.

The effect of the failure of density scaling during the expansion can be made clear by scaling the HANE expansion of Table 1 to the size of a laser experiment. If we maintain the values of temperature and density,

6

but alter t and R by a factor of 10^{-4}, all ξ's will be reduced by this factor. The ζ's will then be at most of order 1. They drop below unity at a density $\sim 10^{18} cm^{-3}$. Thus, the charge state freezes at $10 > z > 6$, as the plasma falls out of equilibrium. The scaling of ξ, by itself, prevents recombination of the plasma down to $z \sim 1$, as in a HANE.

Now, we consider an idealized laser experiment, shown in Table 2 and defined as follows. Starting with the HANE parameters of Table 1, scale time and expansion radius by 10^{-4}. Density drops as in HANE according to a spherical expansion with constant velocity. Assume, however, that temperature is maintained at 500 eV to about 5 nsec. Thereafter, it drops adiabatically. The constant high temperature is due to the continued laser energy deposition. This provides a rough approximation to a laser experiment.

TABLE 2

T (ev)	n_{-3} (cm^{-3})	t (sec)	R (cm)	ξ_{R3}	ξ_{RR}	ξ_{RD}	ξ_I	z
5.0E+02	1.0E+21	4.6E-10	4.6E-02	6.1E-02	3.5E+00	7.4E-01	1.6E+02	11
5.0E+02	1.0E+20	1.0E-09	1.0E-01	1.3E-03	7.5E-01	1.6E-01	3.4E+01	11
5.0E+02	1.0E+19	2.2E-09	2.2E-01	2.8E-05	1.6E-01	3.4E-02	7.3E+00	11
5.0E+02	1.0E+18	4.6E-09	4.6E-01	6.1E-07	3.5E-02	7.4E-03	1.6E+00	11
1.1E+02	1.0E+17	1.0E-08	1.0E+00	3.4E-06	2.7E-02	8.6E-07	7.6E-03	11
2.3E-01	1.0E+16	2.2E-08	2.2E+00	2.8E-04	2.1E-02	0.0E+00	2.8E-10	11
5.0E+00	1.0E+15	4.6E-08	4.6E+00	1.8E-02	1.6E-02	0.0E+00	0.0E+00	11
1.1E+00	1.0E+14	1.0E-07	1.0E+01	2.0E-01	1.2E-02	0.0E+00	0.0E+00	11
2.3E-01	1.0E+13	2.2E-07	2.2E+01	1.2E+00	9.6E-03	0.0E+00	0.0E+00	11

The first table entry shown is for an ion density of 10^{21} cm^{-3}. Maximum heating takes place at electron densities $\sim 10^{21}$ cm^{-3}. Although the laser does not penetrate to higher electron densities thermal conduction maintains the high temperature in the first table entry.

From Table 2 the plasma is in equilibrium at a temperature of 500 eV with $z \geq 11$ as the dominant charge state. When the temperature begins to drop, at densities $\leq 10^{18}$ cm^{-3}, the ξ's for recombination are less than unity. The expansion has reduced densities too much to allow for effective recombination at these temperatures. Eventually, when the temperature drops to very low values (< 1 eV) corresponding to a density $\sim 10^{13}$ cm^{-3}, 3-body recombination would reduce the z value of the debris. Once again, in the real laser experiment recombination will release energy to the electrons, maintaining a higher temperature and suppressing recombination. Furthermore, in the real laser experiment an ambient background gas will stop the expansion, halting the temperature decline. From that point the operative scaling becomes that of Eq. 1. We note, finally, that if in Table 2 we maintained the temperature and density values but scaled t and R by a factor of 10^4, the ξ's would be increased by that factor. Clearly, recombination to lower charge states would rapidly ensue. A HANE size laser experiment would recombine.

IV. Discussion and Conclusion

We compare the above results to a HANEX code simulation of the laser experiment. The state of aluminum target ions without the effects of background coupling was obtained by running the HANEX code with a background nitrogen density of 10^{-6} Torr. The target contained 40 cells, 13 of which blow off the front side. The initial conditions were chosen to match the series of shots described in the experimental coupling study of

Ripin, et al.[6]   The target was 5.6 micron thick aluminum foil. The laser pulse length was 10 nsec with a full width half maximum of 4 nsec. The nominal laser energy was 100 joules with 50 joules within a radius of 125 microns. This produced a forward debris mass of 0.2 micrograms in a cone of half angle 40 degrees. In Table 3 we present the time history of a representative cell with an outward velocity of 5.2 x 10^7 cm/sec . For comparison $\xi_R = \xi_{RR} + \xi_{RD} + \xi_{R3}$ and ξ_I were calculated using the same rates as used for Table 2. The average charge state, $\bar{z} = N_e/n$, is given.

TABLE 3

t (nsec)	R (cm)	n (cm^{-3})	N_e (cm^{-3})	T (ev)	T_e (ev)	ξ_R	ξ_I	$\bar{z}$
3.38	-0.002	6.5E+20	7.0E+21	200.	211.	1.0E+02	1.6E+02	10.8
3.90	0.002	1.5E+20	1.7E+21	453.	489.	5.5E+00	1.9E+02	11.1
4.42	0.012	5.8E+19	6.5E+20	482.	573.	2.2E+00	1.0E+02	11.2
4.91	0.026	1.9E+19	2.1E+20	382.	590.	7.9E-01	3.8E+0	11.3
5.32	0.044	7.1E+18	8.0E+19	293.	570.	3.3E-01	1.5E+01	11.3
5.81	0.062	3.5E+18	3.9E+19	235.	550.	1.8E-01	7.8E+00	11.3
6.55	0.097	1.4E+18	1.5E+19	170.	478.	8.6E-02	2.9E+00	11.3
8.16	0.174	3.8E+17	4.3E+18	105.	269.	4.1E-02	4.0E-01	11.3
11.9	0.384	5.9E+16	6.6E+17	48.	76.	2.6E-02	8.7E-04	11.2
31.5	1.441	1.6E+15	1.7E+16	6.	7.	3.7E-02	1.1E-24	11.2
54.4	2.699	2.5E+14	2.8E+15	2.	2.	2.2E-01	1.7E-25	11.2

At early times when the laser pulse is still on, the ion and electron densities fall due to expansion but the electron temperature stays high first because the laser energy is being absorbed, and then, because of electron thermal conduction from the region of the target that is still

being heated. These effects were accounted for in Table 2 by assuming a constant temperature of 500 ev during the laser pulse. The debris expansion velocity is about a factor of 2 smaller than that of Table 2. This only changes the time scale for expansion by that amount, so Table 3 can be compared directly if time (t) and the ξ's in Table 2 are increased by a factor of 2. We can see that after the laser is turned off (~ 10 nsec) the forward moving debris expands and cools adiabatically, as in our models.

The HANEX code includes laser absorption, radiation transport, time dependent chemistry, thermal conduction, etc. The agreement between code results and the simple models presented in Table 2 after the end of the laser pulse demonstrates that the controlling factors after 10 nsec are, in fact, adiabatic expansion and the recombination rates we discussed.

In conclusion, the simple model calculations given in Section III illustrate the essential differences between HANE and the laser experiment: a low debris charge state in the former and a high charge state in the latter. The primary effect follows from the breakdown of density scaling in the early debris expansion. A secondary effect is a result of the long deposition time of the laser energy, maintaining a higher temperature in the laser experiment than in a HANE at the same densities, even though at earliest times HANE temperatures are higher. We note that the results are essentially unchanged if we reduce this temperature even by a factor of 2 or 3. Recall, that even a scaled down HANE, in which the temperatures are an order of magnitude lower at corresponding densities still resulted in 10 $\geq z > 6$. That is, the primary effect is the debris density scaling breakdown. Finally, we may ask to what extent charge exchange with an ambient background will reduce the debris charge state. We will present detailed simulation results in a separate report. However, we believe that

10

at high background density (0.5 - 5. Torr), where mixing of debris and background is limited, high charge states will persist. At lower background density (0.01 - 0.5 Torr) charge exchange may substantially reduce the charge states.

Acknowledgments

References

1. Clark, R. and V. Jacobs, unpublished.

2. B.H. Ripin, A.W. Ali, H.R. Griem, J. Grun, S.T. Kacenjar, C.K. Manka, E.A. McLean, A.N. Mostovych, S.P. Obenschain, J.A. Stamper, in Laser Interaction & Related Plasma Phenomena, Vol. 7, p. 857-877, ed. by H. Hora & G. Miley, Plenum 1986.

3. Giuliani, J.L. and M. Mulbrandon, "Numerical Simulations of the Laser-Target Interaction and Blast Wave Formation in the DNA/NRL Laser Experiment," NRL Memo No. 5762, 1986.

4. Longmire, C., M. Alme, R. Kilb, L. Wright, "Scaling of Debris-Air Coupling," MRC Report AMRC-R-338(1981).

5. See e.g., Zel'dovich and Raizer, "Physics of Shock Waves and High-Temperature Hydrodynamic Phenomena," Vol. I, Academic Press (1966), equation 6.104.

6. Ripin, B.H., E.A. McLean, J.H. Stamper, J. Grun, C.K. Manka, A.N. Mostovych, "Loss of Collisional Blast Wave Coupling with Pressure," ETHANL 7, 24 (1987).

Appendix I

The rate coefficients for aluminum used to calculate the ξ's for Tables 1 and 2 are given by the following expressions:

Recombination $z \to z - 1$:

$$\alpha_{RR} = A_R \, T_e^{-\eta}$$

$$\alpha_{RD} = A_D e^{-\left(\frac{E1_D}{T_e}\right)} \left[1 + B_D e^{-\left(\frac{E2_D}{T_e}\right)}\right] / T_e^{3/2}$$

$$\alpha_{R3} = MAX(\alpha L_{R3}, \, \alpha H_{R3}), \text{ where}$$

$$\alpha L_{R3} = \frac{8.75 \times 10^{-27} z^3}{T_e^{9/2}} N_e \, MIN\left[1, \, \frac{E_\infty}{100 T_e}\right] \quad \text{(low temperature)}$$

$$\alpha H_{R3} = \frac{N_e \, e^{\left(\frac{E_\infty}{T_e}\right)}}{6 \times 10^{21} T_e^{3/2}} \alpha_I \quad \text{(high temperature)}$$

Ionization $z - 1 \to z$:

$$\alpha_I = \frac{A_I \, x \, e^{-x}}{(x + B_I)} \, , \qquad \text{with} \quad x = \frac{E_I}{T_e}$$

Here T_e is in ev, the α's are in cm^3/sec and E_∞ is the ionization energy of the $z - 1$ ion in ev. The other constants are given in the following table.

z	A_R	η	A_D	B_D	$E1_D$	$E2_D$	A_I	B_I	E_I
1	3.8E-13	7.9E-01	9.6E-10	2.0E-01	2.0E+00	6.0E-01	2.4E-06	0.0E+00	6.0E+00
2	2.1E-12	6.9E-01	2.5E-09	3.0E-01	2.9E+00	4.9E+00	2.8E-07	1.5E-01	1.9E+01
3	3.7E-12	8.2E-01	3.7E-09	0.0E+00	4.1E+01	0.0E+00	6.1E-08	2.3E-02	2.8E+01
4	8.7E-12	7.4E-01	6.2E-10	1.4E+01	2.8E+01	5.5E+01	8.0E-09	1.4E-01	1.2E+02
5	1.6E-11	7.2E-01	1.5E-09	1.1E+00	3.0E+01	7.7E+01	5.3E-09	1.3E-01	1.5E+02
6	2.4E-11	7.0E-01	2.6E-09	1.0E+00	3.1E+01	8.9E+01	2.6E-09	1.1E-01	1.9E+02
7	3.3E-11	6.9E-01	3.8E-08	8.0E-01	3.2E+01	1.2E+02	1.4E-09	1.2E-01	2.4E+02
8	4.9E-11	7.0E-01	2.2E-08	1.6E+01	2.7E+01	1.5E+02	7.0E-10	8.4E-02	2.8E+02
9	6.5E-11	7.1E-01	4.5E-08	5.2E+00	3.0E+01	1.7E+02	3.6E-10	3.0E-02	3.3E+02
10	1.1E-10	8.6E-01	1.3E-08	1.3E+01	1.8E+01	2.2E+02	2.3E-10	2.4E-01	4.0E+02
11	1.2E-10	8.3E-01	2.4E-08	0.0E+00	1.3E+03	0.0E+00	8.6E-11	2.1E-01	4.4E+02
12	1.8E-10	7.6E-01	7.9E-09	3.4E+01	2.5E+02	1.2E+03	5.3E-11	3.4E-01	2.1E+03
13	2.4E-10	7.5E-01	0.0E+00	0.0E+00	0.0E+00	0.0E+00	2.1E-11	3.4E-01	2.3E+03

In the HANEX code (but not in the calculations of ξ in Tables 1-3) the dielectronic recombination rates are reduced to account for density effects. Also, in the code only αH_{R3} is used for 3 body recombination because we do not encounter conditions in our high density background runs where αL_{R3} is important.

DEPARTMENT OF DEFENSE

ASSISTANT SECRETARY OF DEFENSE
COMM, CMD, CONT 7 INTELL
WASHINGTON, DC 20301

DIRECTOR
COMMAND CONTROL TECHNICAL CENTER
PENTAGON RM BE 685
WASHINGTON, DC 20301
  01CY ATTN C-650
  01CY ATTN C-312 R. MASON

DIRECTOR
DEFENSE ADVANCED RSCH PROJ AGENCY
ARCHITECT BUILDING
1400 WILSON BLVD.
ARLINGTON, VA 22209
  01CY ATTN NUCLEAR
      MONITORING RESEARCH
  01CY ATTN STRATEGIC TECH OFFICE

DEFENSE COMMUNICATION ENGINEER CENTER
1860 WIEHLE AVENUE
RESTON, VA 22090
  01CY ATTN CODE R410
  01CY ATTN CODE R812

DIRECTOR
DEFENSE NUCLEAR AGENCY
WASHINGTON, DC 20305
  01CY ATTN STVL
  04CY ATTN TITL
  01CY ATTN DDST
  03CY ATTN RAAE

COMMANDER
FIELD COMMAND
DEFENSE NUCLEAR AGENCY
KIRTLAND, AFB, NM 87115
  01CY ATTN FCPR

DEFENSE NUCLEAR AGENCY
SAO/DNA
BUILDING 20676
KIRTLAND AFB, NM 87115
  01CY D.C. THORNBURG

DIRECTOR
INTERSERVICE NUCLEAR WEAPONS SCHOOL
KIRTLAND AFB, NM 87115
  01CY ATTN DOCUMENT CONTROL

JOINT PROGRAM MANAGEMENT OFFICE
WASHINGTON, DC 20330
  01CY ATTN J-3 WWMCCS EVALUATION
        OFFICE

DIRECTOR
JOINT STRAT TGT PLANNING STAFF
OFFUTT AFB
OMAHA, NB 68113
  01CY ATTN JSTPS/JLKS
  01CY ATTN JPST G. GOETZ

CHIEF
LIVERMORE DIVISION FLD COMMAND DNA
DEPARTMENT OF DEFENSE
LAWRENCE LIVERMORE LABORATORY
P.O. BOX 808
LIVERMORE, CA 94550
  01CY ATTN FCPRL

COMMANDANT
NATO SCHOOL (SHAPE)
APO NEW YORK 09172
  01CY ATTN U.S. DOCUMENTS OFFICER

UNDER SECY OF DEF FOR RSCH & ENGRG
DEPARTMENT OF DEFENSE
WASHINGTON, DC 20301
  01CY ATTN STRATEGIC & SPACE
        SYSTEMS (OS)

COMMANDER/DIRECTOR
ATMOSPHERIC SCIENCES LABORATORY
U.S. ARMY ELECTRONICS COMMAND
WHITE SANDS MISSILE RANGE, NM 88002
  01CY ATTN DELAS-EO, F. NILES

DIRECTOR
BMD ADVANCED TECH CTR
HUNTSVILLE OFFICE
P.O. BOX 1500
HUNTSVILLE, AL 35807
  01CY ATTN ATC-T MELVIN T. CAPPS
  01CY ATTN ATC-O W. DAVIES
  01CY ATTN ATC-R DON RUSS

15

PROGRAM MANAGER
BMD PROGRAM OFFICE
5001 EISENHOWER AVENUE
ALEXANDRIA, VA 22333
  01CY ATTN DACS-BMT J. SHEA

CHIEF C-E- SERVICES DIVISION
U.S. ARMY COMMUNICATIONS CMD
PENTAGON RM 1B269
WASHINGTON, DC 20310
  01CY ATTN C- E-SERVICES DIVISION

COMMANDER
U.S. ARMY COMM-ELEC ENGRG INSTAL AGY
FT. HUACHUCA, AZ 85613
  01CY ATTN CCC-EMEO GEORGE LANE

COMMANDER
U.S. ARMY FOREIGN SCIENCE & TECH CTR
220 7TH STREET, NE
CHARLOTTESVILLE, VA 22901
  01CY ATTN DRXST-SD

COMMANDER
U.S. ARMY MATERIAL DEV & READINESS CMD
5001 EISENHOWER AVENUE
ALEXANDRIA, VA 22333
  01CY ATTN DRCLDC J.A. BENDER

COMMANDER
U.S. ARMY NUCLEAR AND CHEMICAL AGENCY
7500 BACKLICK ROAD
BLDG 2073
SPRINGFIELD, VA 22150
  01CY ATTN LIBRARY

DIRECTOR
U.S. ARMY BALLISTIC RESEARCH
LABORATORY
ABERDEEN PROVING GROUND, MD 21005
  01CY ATTN TECH LIBRARY,
      EDWARD BAICY

COMMANDER
U.S. ARMY SATCOM AGENCY
FT. MONMOUTH, NJ 07703
  01CY ATTN DOCUMENT CONTROL

COMMANDER
U.S. ARMY MISSILE INTELLIGENCE AGENCY
REDSTONE ARSENAL, AL 35809
  01CY ATTN JIM GAMBLE

DIRECTOR
U.S. ARMY TRADOC SYSTEMS ANALYSIS
ACTIVITY
WHITE SANDS MISSILE RANGE, NM 88002
  01CY ATTN ATAA-SA
  01CY ATTN TCC/F. PAYAN JR.
  01CY ATTN ATTA-TAC LTC J. HESSE

COMMANDER
NAVAL ELECTRONIC SYSTEMS COMMAND
WASHINGTON, DC 20360
  01CY ATTN NAVALEX 034 T. HUGHES
  01CY ATTN PME 117
  01CY ATTN PME 117-T
  01CY ATTN CODE 5011

COMMANDING OFFICER
NAVAL INTELLIGENCE SUPPORT CTR
4301 SUITLAND ROAD, BLDG. 5
WASHINGTON, DC 20390
  01CY ATTN MR. DUBBIN STIC 12
  01CY ATTN NISC-50
  01CY ATTN CODE 5404 J. GALET

COMMANDER
NAVAL OCEAN SYSTEMS CENTER
SAN DIEGO, CA 92152
  01CY ATTN J. FERGUSON

NAVAL RESEARCH LABORATORY
WASHINGTON, DC 20375
  01CY ATTN CODE 4700 S.L. Ossakow,
        26 CYS IF UNCLASS
        (01CY IF CLASS)
        ATTN CODE 4780 J.D. HUBA, 50
        CYS IF UNCLASS, 01CY IF CLASS
  01CY ATTN CODE 4701 I. VITKOVITSKY
  01CY ATTN CODE 7500
  01CY ATTN CODE 7550
  01CY ATTN CODE 7580
  01CY ATTN CODE 7551
  01CY ATTN CODE 7555
  01CY ATTN CODE 4730 E. MCLEAN
  01CY ATTN CODE 4752
  01CY ATTN CODE 4730 B. RIPIN
  20CY ATTN CODE 2628

COMMANDER
NAVAL SPACE SURVEILLANCE SYSTEM
DAHLGREN, VA 22448
  01CY ATTN CAPT J.H. BURTON

OFFICER-IN-CHARGE
NAVAL SURFACE WEAPONS CENTER
WHITE OAK, SILVER SPRING, MD 20910
  01CY   ATTN CODE F31

DIRECTOR
STRATEGIC SYSTEMS PROJECT OFFICE
DEPARTMENT OF THE NAVY
WASHINGTON, DC 20376
  01CY   ATTN NSP-2141
  01CY   ATTN NSSP-2722   FRED WIMBERLY

COMMANDER
NAVAL SURFACE WEAPONS CENTER
DAHLGREN LABORATORY
DAHLGREN, VA 22448
  01CY   ATTN CODE DF-14   R. BUTLER

OFFICER OF NAVAL RESEARCH
ARLINGTON, VA 22217
  01CY   ATTN CODE 465
  01CY   ATTN CODE 461
  01CY   ATTN CODE 402
  01CY   ATTN CODE 420
  01CY   ATTN CODE 421

COMMANDER
AEROSPACE DEFENSE COMMAND/XPD
DEPARTMENT OF THE AIR FORCE
ENT AFB, CO 80912
  01CY   ATTN XPDQQ
  01CY   ATTN XP

AIR FORCE GEOPHYSICS LABORATORY
HANSCOM AFB, MA 01731
  01CY   ATTN OPR   HAROLD GARDNER
  01CY   ATTN LKB
         KENNETH S.W. CHAMPION
  01CY   ATTN OPR   ALVA T. STAIR
  01CY   ATTN PHD   JURGEN BUCHAU
  01CY   ATTN PHD   JOHN P. MULLEN

AF WEAPONS LABORATORY
KIRTLAND AFB, NM 87117
  01CY   ATTN SUL
  01CY   ATTN CA   ARTHUR H. GUENTHER

AFTAC
PATRICK AFB, FL 32925
  01CY   ATTN TN

AIR FORCE AVIONICS LABORATORY
WRIGHT-PATTERSON AFB, OH 45433
  01CY   ATTN AAD   WADE HUNT
  01CY   ATTN AAD   ALLEN JOHNSON

DEPUTY CHIEF OF STAFF
RESEARCH, DEVELOPMENT, & ACQ
DEPARTMENT OF THE AIR FORCE
WASHINGTON, DC 20330
  01CY   ATTN AFRDQ

HEADQUARTERS
ELECTRONIC SYSTEMS DIVISION
DEPARTMENT OF THE AIR FORCE
HANSCOM AFB, MA 01731-5000
  01CY   ATTN J. DEAS
         ESD/SCD-4

COMMANDER
FOREIGN TECHNOLOGY DIVISION, AFSC
WRIGHT-PATTERSON AFB, OH 45433
  01CY   ATTN NICD   LIBRARY
  01CY   ATTN ETDP   B. BALLARD

COMMANDER
ROME AIR DEVELOPMENT CENTER, AFSC
GRIFFISS AFB, NY 13441
  01CY   ATTN DOC LIBRARY/TSLD
  01CY   ATTN OCSE   V. COYNE

STRATEGIC AIR COMMAND/XPFS
OFFUTT AFB, NB 68113
  01CY   ATTN XPFS

SAMSO/MN
NORTON AFB, CA 92409
(MINUTEMAN)
  01CY   ATTN MNNL

COMMANDER
ROME AIR DEVELOPMENT CENTER, AFSC
HANSCOM AFB, MA 01731
  01CY   ATTN EEP   A. LORENTZEN

DEPARTMENT OF ENERGY
LIBRARY ROOM G-042
WASHINGTON, DC 20545
  01CY   ATTN DOC CON FOR A. LABOWITZ

DEPARTMENT OF ENERGY
ALBUQUERQUE OPERATIONS OFFICE
P.O. BOX 5400
ALBUQUERQUE, NM 87115
  01CY   ATTN DOC CON FOR D. SHERWOOD

17

EG&G, INC.
LOS ALAMOS DIVISION
P.O. BOX 809
LOS ALAMOS, NM 85544
  01CY   ATTN DOC CON FOR J. BREEDLOVE

UNIVERSITY OF CALIFORNIA
LAWRENCE LIVERMORE LABORATORY
P.O. BOX 808
LIVERMORE, CA 94550
  01CY   ATTN DOC CON FOR TECH INFO
         DEPT
  01CY   ATTN DOC CON FOR L-389 R. OTT
  01CY   ATTN DOC CON FOR L-31 R. HAGER

LOS ALAMOS NATIONAL LABORATORY
P.O. BOX 1663
LOS ALAMOS, NM 87545
  01CY   ATTN DOC CON FOR J. WOLCOTT
  01CY   ATTN DOC CON FOR R.F. TASCHEK
  01CY   ATTN DOC CON FOR E. JONES
  01CY   ATTN DOC CON FOR J. MALIK
  01CY   ATTN DOC CON FOR R. JEFFRIES
  01CY   ATTN DOC CON FOR J. ZINN
  01CY   ATTN DOC CON FOR D. WESTERVELT
  01CY   ATTN D. SAPPENFIELD

LOS ALAMOS NATIONAL LABORATORY
MS D438
LOS ALAMOS, NM 87545
  01CY   ATTN S.P. GARY
  01CY   ATTN J. BOROVSKY

SANDIA LABORATORIES
P.O. BOX 5800
ALBUQUERQUE, NM 87115
  01CY   ATTN DOC CON FOR W. BROWN
  01CY   ATTN DOC CON FOR A.
         THORNBROUGH
  01CY   ATTN DOC CON FOR T. WRIGHT
  01CY   ATTN DOC CON FOR D. DAHLGREN
  01CY   ATTN DOC CON FOR 3141
  01CY   ATTN DOC CON FOR SPACE PROJECT
         DIV

SANDIA LABORATORIES
LIVERMORE LABORATORY
P.O. BOX 969
LIVERMORE, CA 94551
  01CY   ATTN DOC CON FOR B. MURPHEY
  01CY   ATTN DOC CON FOR T. COOK

OFFICE OF MILITARY APPLICATION
DEPARTMENT OF ENERGY
WASHINGTON, DC 20545
  01CY   ATTN DOC CON DR. YO SONG

NATIONAL OCEANIC & ATMOSPHERIC ADMIN
ENVIRONMENTAL RESEARCH LABORATORIES
DEPARTMENT OF COMMERCE
BOULDER, CO 80302
  01CY   ATTN R. GRUBB

DEPARTMENT OF DEFENSE CONTRACTORS

AEROSPACE CORPORATION
P.O. BOX 92957
LOS ANGELES, CA 90009
  01CY   ATTN I. GARFUNKEL
  01CY   ATTN T. SALMI
  01CY   ATTN V. JOSEPHSON
  01CY   ATTN S. BOWER
  01CY   ATTN D. OLSEN

ANALYTICAL SYSTEMS ENGINEERING CORP
5 OLD CONCORD ROAD
BURLINGTON, MA 01803
  01CY   ATTN RADIO SCIENCES

AUSTIN RESEARCH ASSOC., INC.
1901 RUTLAND DRIVE
AUSTIN, TX 78758
  01CY   ATTN L. SLOAN
  01CY   ATTN R. THOMPSON

BERKELEY RESEARCH ASSOCIATES, INC.
P.O. BOX 983
BERKELEY, CA 94701
  01CY   ATTN J. WORKMAN
  01CY   ATTN C. PRETTIE
  01CY   ATTN S. BRECHT

BOEING COMPANY, THE
P.O. BOX 3707
SEATTLE, WA 98124
  01CY   ATTN G. KEISTER
  01CY   ATTN D. MURRAY
  01CY   ATTN G. HALL
  01CY   ATTN J. KENNEY

CHARLES STARK DRAPER LABORATORY, INC
555 TECHNOLOGY SQUARE
CAMBRIDGE, MA 02139
  01CY   ATTN D.B. COX
  01CY   ATTN J.P. GILMORE

COMSAT LABORATORIES
22300 COMSAT DRIVE
CLARKSBURG, MD 20871
  01CY   ATTN G. HYDE

CORNELL UNIVERSITY
DEPARTMENT OF ELECTRICAL ENGINEERING
ITHACA, NY 14850
  01CY   ATTN D.T. FARLEY, JR.

ELECTROSPACE SYSTEMS, INC.
BOX 1359
RICHARDSON, TX 75080
  01CY   ATTN H. LOGSTON
  01CY   ATTN SECURITY (PAUL PHILLIPS)

EOS TECHNOLOGIES, INC.
606 Wilshire Blvd.
Santa Monica, CA 90401
  01CY   ATTN C.B. GABBARD
  01CY   ATTN R. LELEVIER

GENERAL ELECTRIC COMPANY
SPACE DIVISION
VALLEY FORGE SPACE CENTER
GODDARD BLVD KING OF PRUSSIA
P.O. BOX 8555
PHILADELPHIA, PA 19101
  01CY   ATTN M.H. BORTNER
         SPACE SCI LAB

GEOPHYSICAL INSTITUTE
UNIVERSITY OF ALASKA
FAIRBANKS, AK 99701
  (ALL CLASS ATTN: SECURITY OFFICER)
  01CY   ATTN T.N. DAVIS (UNCLASS ONLY)
  01CY   ATTN NEAL BROWN (UNCLASS ONLY)

GTE SYLVANIA, INC.
ELECTRONICS SYSTEMS GRP-EASTERN DIV
77 A STREET
NEEDHAM, MA 02194
  01CY   ATTN DICK STEINHOF

HSS, INC.
2 ALFRED CIRCLE
BEDFORD, MA 01730
  01CY   ATTN DONALD HANSEN

ILLINOIS, UNIVERSITY OF
107 COBLE HALL
150 DAVENPORT HOUSE
CHAMPAIGN, IL 61820
  (ALL CORRES ATTN DAN MCCLELLAND)
  01CY ATTN K. YEH

INSTITUTE FOR DEFENSE ANALYSES
1801 NO. BEAUREGARD STREET
ALEXANDRIA, VA 22311
  01CY   ATTN J.M. AEIN
  01CY   ATTN ERNEST BAUER
  01CY   ATTN HANS WOLFARD
  01CY   ATTN JOEL BENGSTON

INTL TEL & TELEGRAPH CORPORATION
500 WASHINGTON AVENUE
NUTLEY, NJ 07110
  01CY   ATTN TECHNICAL LIBRARY

JAYCOR
11011 TORREYANA ROAD
P.O. BOX 85154
SAN DIEGO, CA 92138
  01CY   ATTN J.L. SPERLING

JOHNS HOPKINS UNIVERSITY
APPLIED PHYSICS LABORATORY
JOHNS HOPKINS ROAD
LAUREL, MD 20810
  01CY   ATTN DOCUMENT LIBRARIAN
  01CY   ATTN THOMAS POTEMRA
  01CY   ATTN JOHN DASSOULAS

KAMAN SCIENCES CORP
P.O. BOX 7463
COLORADO SPRINGS, CO 80933
  01CY   ATTN T. MEAGHER

KAMAN TEMPO-CENTER FOR ADVANCED
STUDIES
816 STATE STREET (P.O DRAWER QQ)
SANTA BARBARA, CA 93102
  01CY   ATTN DASIAC
  01CY   ATTN WARREN S. KNAPP
  01CY   ATTN WILLIAM MCNAMARA
  01CY   ATTN B. GAMBILL

LINKABIT CORP
10453 ROSELLE
SAN DIEGO, CA 92121
  01CY   ATTN IRWIN JACOBS

LOCKHEED MISSILES & SPACE CO., INC
P.O. BOX 504
SUNNYVALE, CA 94088
  01CY ATTN DEPT 60-12
  01CY ATTN D.R. CHURCHILL

LOCKHEED MISSILES & SPACE CO., INC.
3251 HANOVER STREET
PALO ALTO, CA 94304
  01CY ATTN MARTIN WALT DEPT 52-12
  01CY ATTN W.L. IMHOF DEPT 52-12
  01CY ATTN RICHARD G. JOHNSON
       DEPT 52-12
  01CY ATTN J.B. CLADIS DEPT 52-12

MARTIN MARIETTA CORP
ORLANDO DIVISION
P.O. BOX 5837
ORLANDO, FL 32805
  01CY ATTN R. HEFFNER

MCDONNEL DOUGLAS CORPORATION
5301 BOLSA AVENUE
HUNTINGTON BEACH, CA 92647
  01CY ATTN N. HARRIS
  01CY ATTN J. MOULE
  01CY ATTN GEORGE MROZ
  01CY ATTN W. OLSON
  01CY ATTN R.W. HALPRIN
  01CY ATTN TECHNICAL
       LIBRARY SERVICES

MISSION RESEARCH CORPORATION
735 STATE STREET
SANTA BARBARA, CA 93101
  01CY ATTN P. FISCHER
  01CY ATTN W.F. CREVIER
  01CY ATTN STEVEN L. GUTSCHE
  01CY ATTN R. BOGUSCH
  01CY ATTN R. HENDRICK
  01CY ATTN RALPH KILB
  01CY ATTN DAVE SOWLE
  01CY ATTN F. FAJEN
  01CY ATTN M. SCHEIBE
  01CY ATTN CONRAD L. LONGMIRE
  01CY ATTN B. WHITE
  01CY ATTN R. STAGAT

MISSION RESEARCH CORP.
1720 RANDOLPH ROAD, S.E.
ALBUQUERQUE, NM 87106
  01CY ATTN L. STOLLINGWERF
  01CY ATTN M. ALME
  01CY ATTN L. WRIGHT

MITRE CORP
WESTGATE RESEARCH PARK
1820 DOLLY MADISON BLVD
MCLEAN, VA 22101
  01CY ATTN W. HALL
  01CY ATTN W. FOSTER

PACIFIC-SIERRA RESEARCH CORP
12340 SANTA MONICA BLVD.
LOS ANGELES, CA 90025
  01CY ATTN E.C. FIELD, JR.

PENNSYLVANIA STATE UNIVERSITY
IONOSPHERE RESEARCH LAB
318 ELECTRICAL ENGINEERING EAST
UNIVERSITY PARK, PA 16802
  (NO CLASS TO THIS ADDRESS)
  01CY ATTN IONOSPHERIC RESEARCH LAB

PHOTOMETRICS, INC.
4 ARROW DRIVE
WOBURN, MA 01801
  01CY ATTN IRVING L. KOFSKY

PHYSICAL DYNAMICS, INC.
P.O. BOX 3027
BELLEVUE, WA 98009
  01CY ATTN E.J. FREMOUW

PHYSICAL DYNAMICS, INC.
P.O. BOX 10367
OAKLAND, CA 94610
  ATTN A. THOMSON

R & D ASSOCIATES
P.O. BOX 9695
MARINA DEL REY, CA 90291
  01CY ATTN FORREST GILMORE
  01CY ATTN WILLIAM B. WRIGHT, JR.
  01CY ATTN WILLIAM J. KARZAS
  01CY ATTN H. ORY
  01CY ATTN C. MACDONALD
  01CY ATTN BRIAN LAMB
  01CY ATTN MORGAN GROVER

RAYTHEON CO.
528 BOSTON POST ROAD
SUDBURY, MA 01776
  01CY ATTN BARBARA ADAMS

RIVERSIDE RESEARCH INSTITUTE
330 WEST 42nd STREET
NEW YORK, NY 10036
  01CY ATTN VINCE TRAPANI

SCIENCE APPLICATIONS
  INTERNATIONAL INCORPORATED
1150 PROSPECT PLAZA
LA JOLLA, CA 92037
  01CY ATTN LEWIS M. LINSON
  01CY ATTN DANIEL A. HAMLIN
  01CY ATTN E. FRIEMAN
  01CY ATTN E.A. STRAKER
  01CY ATTN CURTIS A. SMITH

SCIENCE APPLICATIONS
  INTERNATIONAL CORPORATION
1710 GOODRIDGE DR.
MCLEAN, VA 22102
  01CY J. COCKAYNE
  01CY E. HYMAN

SRI INTERNATIONAL
333 RAVENSWOOD AVENUE
MENLO PARK, CA 94025
  01CY ATTN J. CASPER
  01CY ATTN DONALD NEILSON
  01CY ATTN ALAN BURNS
  01CY ATTN G. SMITH
  01CY ATTN R. TSUNODA
  01CY ATTN DAVID A. JOHNSON
  01CY ATTN WALTER G. CHESNUT
  01CY ATTN CHARLES L. RINO
  01CY ATTN WALTER JAYE
  01CY ATTN J. VICKREY
  01CY ATTN RAY L. LEADABRAND
  01CY ATTN G. CARPENTER
  01CY ATTN G. PRICE
  01CY ATTN R. LIVINGSTON
  01CY ATTN V. GONZALES
  01CY ATTN D. MCDANIEL

TECHNOLOGY INTERNATIONAL CORP
75 WIGGINS AVENUE
BEDFORD, MA 01730
  01CY ATTN W.P. BOQUIST

TRW DEFENSE & SPACE SYS GROUP
ONE SPACE PARK
REDONDO BEACH, CA 90278
  01CY ATTN R. K. PLEBUCH
  01CY ATTN S. ALTSCHULER
  01CY ATTN D. DEE
  01CY ATTN D/ STOCKWELL
        SNTF/1575

VISIDYNE
SOUTH BEDFORD STREET
BURLINGTON, MA 01803
  01CY ATTN W. REIDY
  01CY ATTN J. CARPENTER
  01CY ATTN C. HUMPHREY

UNIVERSITY OF PITTSBURGH
PITTSBURGH, PA 15213
  01CY ATTN: N. ZABUSKY

21

END

Feb.

1988

DTIC